

**Supplemental information**

**Structure and function of persulfide dioxygenase**

**from *Pseudomonas aeruginosa*: Implications on H<sub>2</sub>S**

**homeostasis and interplay with nitric oxide**

**Francesca Giordano, Francesca Troilo, Martina Roberta Nastasi, Lorenzo Caruso, Marta Mellini, Carlo Travaglini-Allocatelli, Giorgio Giardina, João B. Vicente, Giordano Rampioni, Adele Di Matteo, Elena Forte, and Alessandro Giuffrè**

## Supplementary material

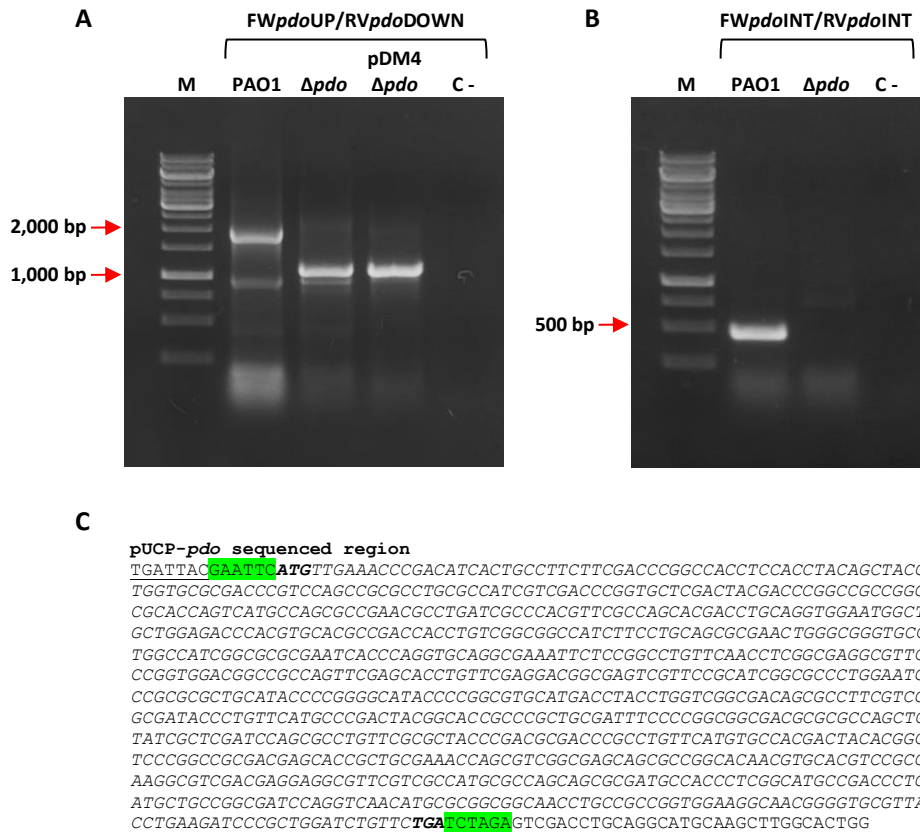


**Figure S1. Validation of the *pdo* mutant and *pdo*-expressing plasmid.** (A) and (B) Gel electrophoresis analysis of PCR products performed to verify the deletion of the *pdo* gene from PAO1 chromosome. (A) Amplicons obtained on the PAO1 and the  $\Delta$ *pdo* chromosomes, or the pDM4 $\Delta$ *pdo* plasmid, by using primers FW*pdo*UP (CCGCTCGAGGTTGCTGCGACGCCATCC) and RV*pdo*DOWN (GCTCTAGAGGCGACCACCGCGCCG). Expected products length was 1,898 bp for PAO1, and 1,080 bp for  $\Delta$ *pdo* and pDM4 $\Delta$ *pdo*. (B) Amplicons obtained on the PAO1 and the  $\Delta$ *pdo* chromosomes by using primers FW*pdo*INT (ATCTTCCTGCAGCGGAAC) and RV*pdo*INT (TCGCGGACGTGCACGTTG). Expected product length was 458 bp for PAO1, while no product was expected in the  $\Delta$ *pdo* mutant as these primers anneal in an internal region of the *pdo* gene. M, molecular weight marker (Generuler 1 kb DNA ladder, GeneDirex); C -, no DNA template added. (C) DNA sequence obtained by Sanger sequencing of the pUCP-*pdo* plasmid using primer RVM13 (CAGGAAACAGCTATGAC), which anneals 26 bp upstream of the EcoRI restriction site in pUCP18. The obtained sequence includes the complete *pdo* gene and a portion of the pUCP18 vector. Alignment between the sequenced plasmid region and the theoretical sequence revealed complete correspondance (verified with the Clustal Omega sequence alignment tool). The pUCP18 sequence is underlined; recognition sites for the EcoRI and XbaI restriction enzymes used for *pdo* cloning into pUCP18 are shaded in green; the *pdo* gene sequence is shown in italics, with start and stop codons in bold

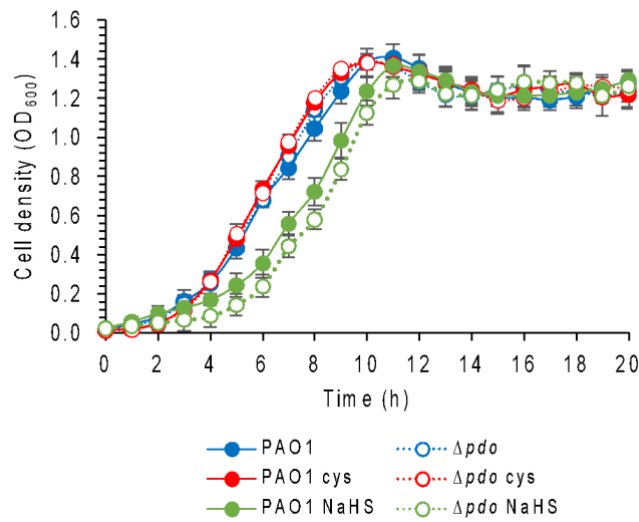


**Figure S2. Growth curves of *P. aeruginosa* PAO1 and its isogenic  $\Delta pdo$  mutant.** Growth curves of *P. aeruginosa* PAO1 (solid lines, full circles) and its isogenic  $\Delta pdo$  mutant (dashed lines, empty circles). Strains were grown in 96-well microtiter plates in LB (blue lines) or in LB supplemented with 200  $\mu$ M L-cysteine (cvs; red lines) or 200  $\mu$ M NaHS (green lines). Mean and standard deviations

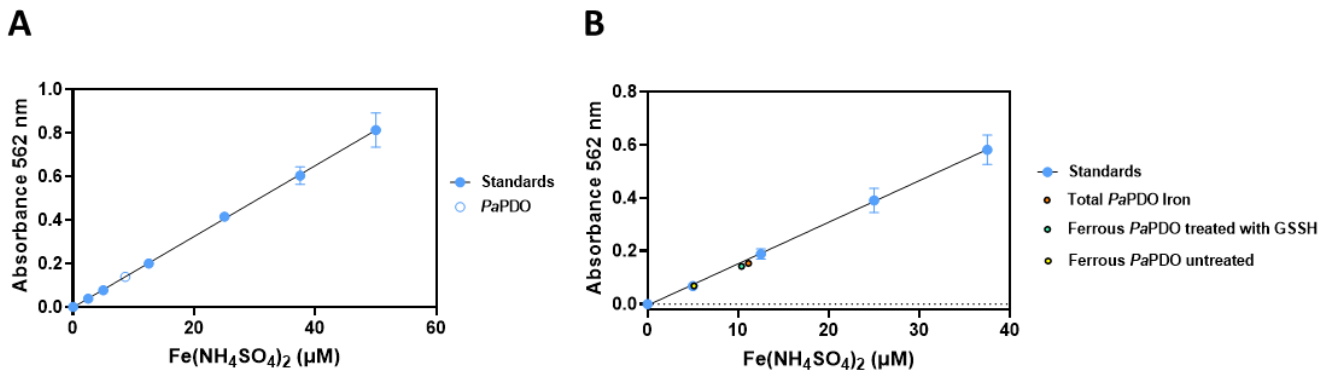


**Figure S3. Ferrozine Assay for Iron quantification of *PaPDO*.** Standard curve: solid blue circles represent the absorbance at 562 nm measured for increasing concentrations of  $Fe^{2+}$  (as  $Fe(NH_4SO_4)_2$ ) complexed with ferrozine. (A) Total iron content and iron occupancy estimation in the “as-prepared” *PaPDO*. The empty blue circle indicates the interpolated absorbance value corresponding to the total iron content in the *PaPDO* sample. The measured iron concentration (8.3  $\mu$ M), with respect to *PaPDO* monomer concentration (11.3  $\mu$ M), indicates a stoichiometry of approximately 0.7 mol Fe per mol *PaPDO* monomer, i.e. ~70% of the protein is in the holo form. (B) Ferrous iron content in GSSH-treated (green circle) and untreated *PaPDO* (yellow circle). *PaPDO* total iron content (orange circle). In the presence of GSSH, the iron is almost fully reduced (11  $\mu$ M total iron, 10.3  $\mu$ M ferrous iron in GSSH-treated *PaPDO* and 5.1  $\mu$ M in the untreated sample).

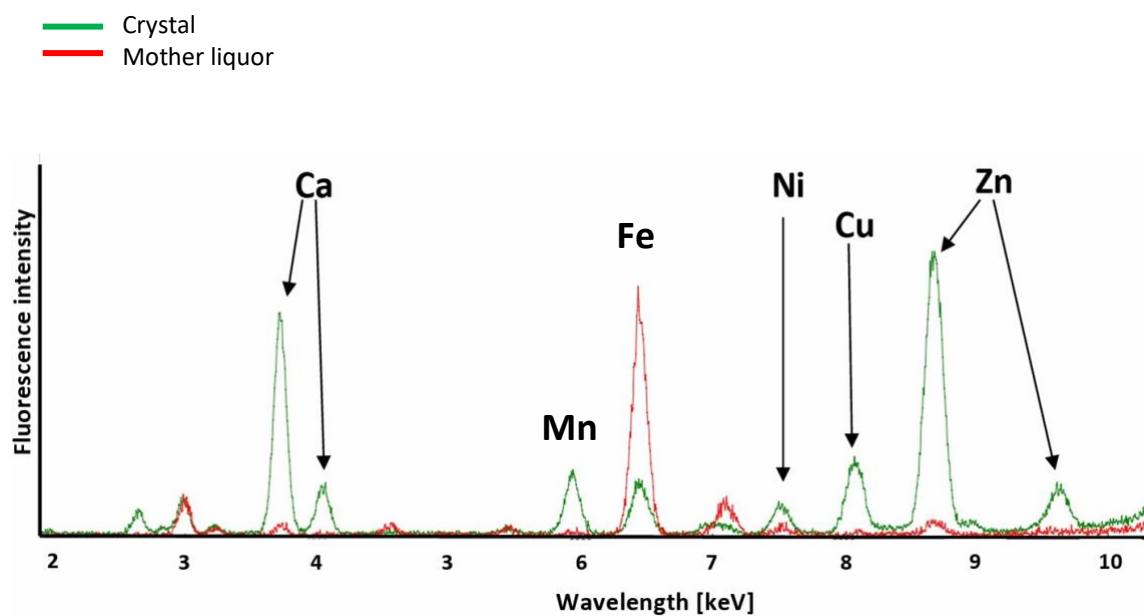


**Figure S4. X-ray fluorescence spectrum of PaPDO crystals.** The emission spectrum of the crystal and the mother liquor are shown in green and red, respectively. Spectra indicates a mixed situation with a prevalence of Zn and Ca ions.

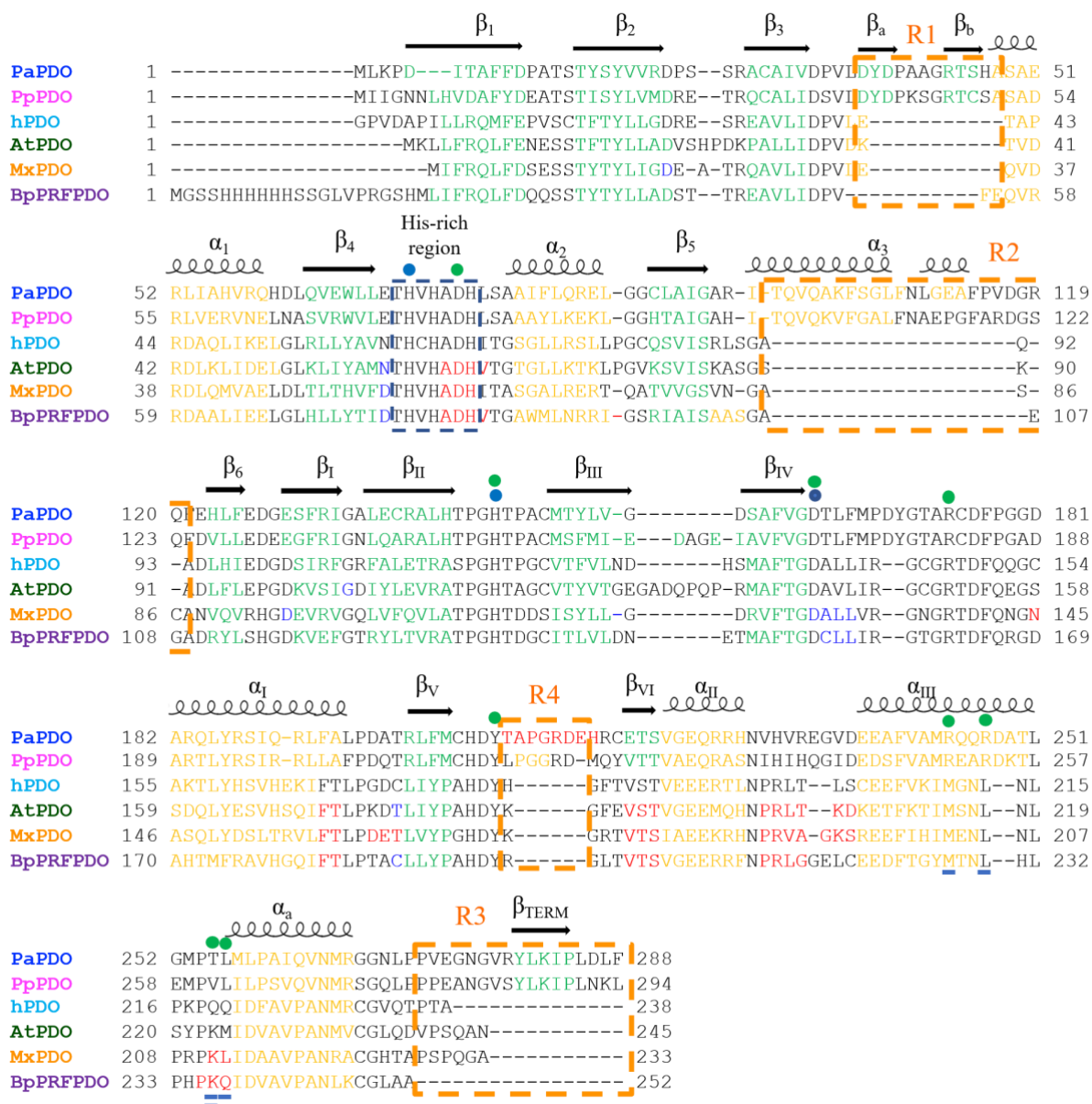


**Figure S5. Sequence comparison of PDO from *P. aeruginosa*, *P. putida* and hPDO.** Sequence comparison of PDO from *P. aeruginosa* (PaPDO, Uniprot: Q9HZT2) *P. putida* (PpPDO, PDB code: 4ysk, Uniprot: A5VWI3), hPDO (hPDO, PDB code: 4chl, Uniprot: O95571), *M. xanthus* (MxPDO, PDB code: 4ysb, Uniprot: Q1D4C9), *A. thaliana* (AtPDO, PDB code: 2gcu, Uniprot: Q9C8L4), *B. phytofirmans* (BpPRF, PDB code: 5ve3, Uniprot: B2TEQ2). The residues involved in the metal coordination are marked with blue dots; the residues involved in the interaction with GSH, according to Sattler et al. 2015 [28], are marked with green dots. Among them, underlined residues are conserved only in *Pa* and *Pp*PDO, the amino acid underlined with 2 lines is not conserved

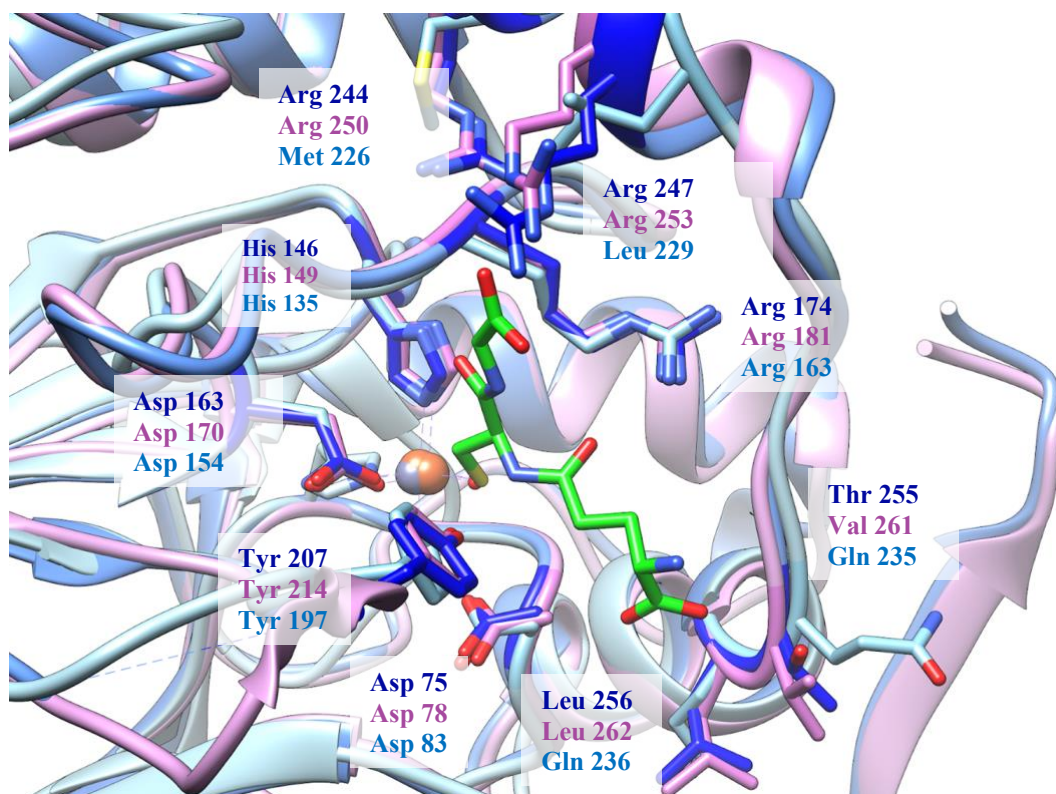


**Figure S6. Comparison of the PDO active sites.** Close view of the active sites of the superposed structures of hPDO (light blue), PaPDO (cornflower blue) and PpPDO (plum) with the substrate (GSH, light green) from PpPDO structure (PDB code: 4ysl). The residues involved in the interaction with GSH, according to Sattler et al. 2015, are represented in light purple in PpPDO, in blue in PaPDO and in light blue in hPDO.

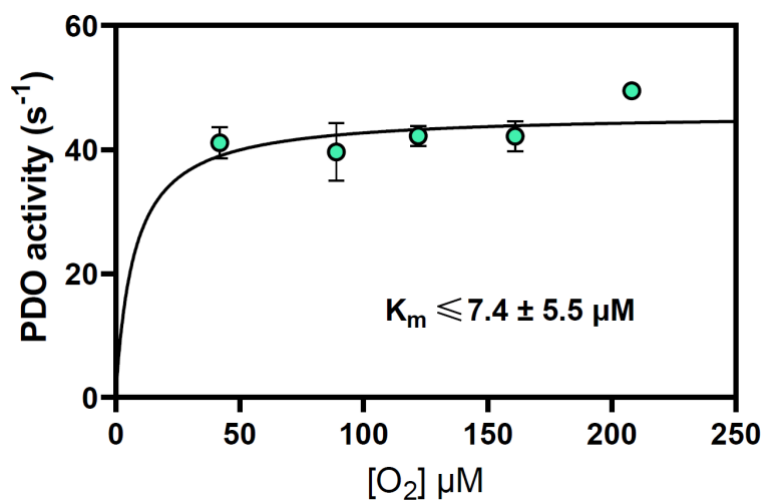


**Figure S7. Apparent Km for oxygen.** PaPDO activity versus O<sub>2</sub> concentration was determined at 25 °C in 100 mM Na phosphate pH 7.4 in the presence of 160 μM GSSH. The activity was determined at different O<sub>2</sub> concentrations (50- 250 μM) obtained by bubbling the solution with N<sub>2</sub> flux for different seconds. PDO activity is about the same for all the O<sub>2</sub> concentrations, the higher limit of the Km (O<sub>2</sub>) was determined.

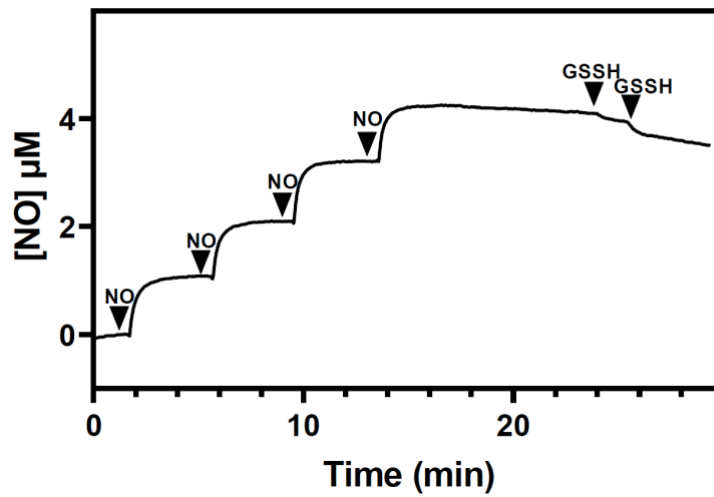


**Figure S8. Effect of GSSH on NO concentration under anaerobic conditions.** Four consecutive aliquots of 1.1 μM NO were added to degassed Na phosphate 100 mM buffer, pH 7.4, in the presence of 1 U/ml ascorbic oxidase and 5 mM ascorbate. The addition of 5 μM and 10 μM GSSH aliquots to the chamber results in a small decrease in NO concentration compared to *Pa*PDO.

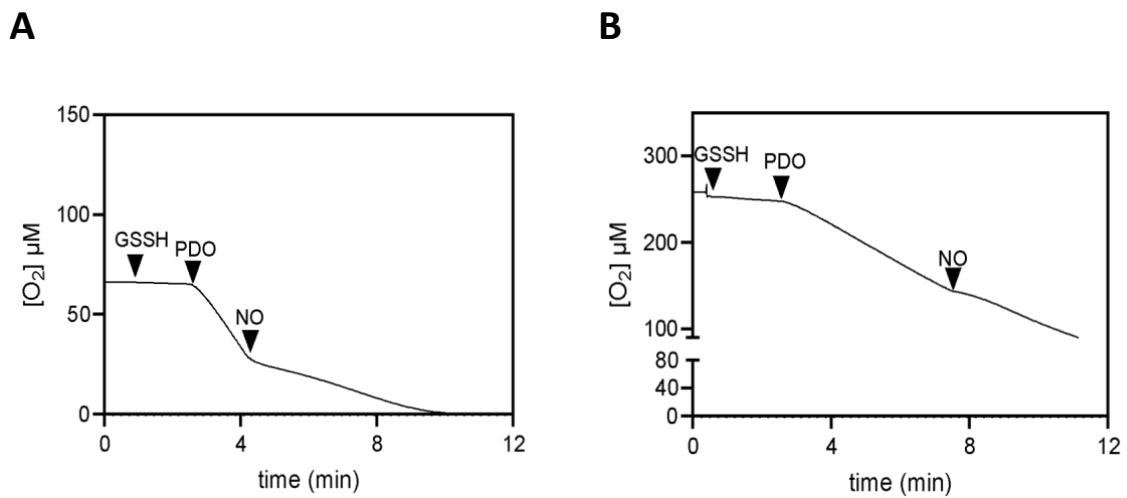


**Figure S9. *Pa*PDO inhibition by NO at low and high oxygen.** Oxygraphic traces of *Pa*PDO (5.3 nM holoprotein) in the presence GSSH (160 μM). (A) 1 μM NO was added at 20 μM oxygen. (B) 1 μM NO was added at 130 μM oxygen. *Pa*PDO was more potently inhibited by NO at low oxygen levels

**Table I.** X-ray data collection and refinement statistics for *Pa*PDO.

<b>Data collection</b>	
Beamline	ELETTRA - XRD2
Wavelength (Å)	1.000
Space group	P 31 2 1
Cell dimensions (Å, °)	77.24 77.24 83.30; 90 90 120
Resolution range (Å)	66.89 – 2.06 (2.14 - 2.06)
CC(1/2)(%)	99.9 (85.5)
Mean I/sigma (I)	18.2 (2.2)
Completeness (%)	100 (100)
Reflections	
Total reflections	317221 (15700)
Multiplicity	17.5 (17.7)
Wilson plot <i>B</i> value	45.7
<b>Refinement</b>	
Resolution range	66.89 – 2.06
<i>R</i> <sub>work</sub> / <i>R</i> <sub>free</sub> *(%)	19.2 (26.3) / 23.9 (30.2)
Average B-factor (Å <sup>2</sup> ) (no. of atoms)	
Overall	61.93 (2285)
Protein	62.01 (2197)
Waters	57.02 (78)
Others	81.90 (10)
RMSD	
Bond length (Å)	0.008
Bond angle (°)	0.910
Ramachandran favoured (%)	
Favoured / Allowed / Outliers	97.09 / 2.91 / 0.00
<b>PDB code</b>	9G8T

*Statistics for the highest-resolution shell are shown in parentheses.*

\* *R*<sub>free</sub> was calculated using 5% of randomly chosen reflection from each resolution shell.